Measurement of the high-field Q drop in the TM_{010} and TE_{011} modes in a niobium cavity

Gianluigi Ciovati[1] and Peter Kneisel[2]

[1]*Thomas Jefferson National Accelerator Facility, Newport News, Virginia 23606, USA, and Department of Physics, Old Dominion University, Norfolk, Virginia 23529, USA*

[2]*Thomas Jefferson National Accelerator Facility, Newport News, Virginia 23606, USA*

(Received 11 February 2006; published 13 April 2006)

In the last few years superconducting radio-frequency (rf) cavities made of high-purity (residual resistivity ratio > 200) niobium achieved accelerating gradients close to the theoretical limits. An obstacle towards achieving reproducibly higher fields is represented by "anomalous" losses causing a sharp degradation of the cavity quality factor when the peak surface magnetic field (B_p) is above about 90 mT, in the absence of field emission. This effect, called "Q drop" has been measured in many laboratories with single- and multicell cavities mainly in the gigahertz range. In addition, a low-temperature (100–140 °C) "*in situ*" baking of the cavity was found to be beneficial in reducing the Q drop. In order to gain some understanding of the nature of these losses, a single-cell cavity has been tested in the TM_{010} and TE_{011} modes at 2 K. The feature of the TE_{011} mode is to have zero electric field on the cavity surface, so that electric field effects can be excluded as a source for the Q drop. This article will present some of the experimental results for different cavity treatments and will compare them with existing models.

DOI: 10.1103/PhysRevSTAB.9.042001 PACS numbers: 74.25.Nf, 84.40.−x

I. INTRODUCTION

A useful technique to investigate the dependence of the surface resistance as a function of the peak surface magnetic field is to excite a single-cell cavity in various resonant modes characterized by different surface field distributions. This provides some insight about the nature and location of the rf losses.

Field emission free superconducting cavities made of bulk niobium show a severe degradation of the quality factor Q_0 at peak magnetic surface fields above about 90 mT. An empirical method that is effective in reducing the Q drop is a low-temperature (100–140 °C) "*in situ*" baking of the cavity in ultrahigh vacuum. The majority of the models that try to describe the Q-drop phenomenon involve a magnetic field effect [1] while a model proposed by Halbritter [2,3] involves an electric field effect. The validity of these models can be tested by measuring a single-cell cavity in the usual TM_{010} mode, used for particle acceleration, and in the TE_{011} mode which has no electric field on the surface. Using properly designed input and output loop couplers it is possible to excite both modes of the cavity at 2 K under ultrahigh vacuum and therefore allows testing both TE and TM mode under the same conditions of the niobium surface. The results presented in this article include different treatments of the niobium cavity, besides the low-temperature baking, which further test the hypothesis of various Q-drop models. In particular, a thick oxide layer can be formed on the niobium surface by anodization and this should lower the onset field for the Q drop, according to the model of Refs. [2,3]. Postpurification of the niobium cavity improves the thermal conductivity of the material, which should reduce the Q drop if it would be caused by the limited heat transfer from the rf surface to the helium bath, as proposed by the so-called thermal feedback model described in Ref. [4].

II. EXPERIMENTAL SETUP AND RESULTS

A. Experimental setup

The cavity used for this experimental study has the same shape as the one used in the CEBAF accelerator [5]. The main electromagnetic parameters of the TM_{010} and TE_{011} mode are shown in Table I as calculated with SUPERFISH [6]. The cavity effective area, A_{eff}, represents the surface area where most of the heat due to rf losses is dissipated. It is defined as [7]

$$A_{\mathrm{eff}} = \frac{\int_S H^2 ds}{H_p^2}. \quad (1)$$

Figure 1 shows the fields distribution on the cavity surface. The TM_{010} mode has high magnetic field in the equator area while the TE_{011} mode has high magnetic field on the

TABLE I. Main parameters of the TM_{010} and TE_{011} modes for a CEBAF single-cell cavity. R_s is the surface resistance, E_p is the peak surface electric field, and U is the stored energy.

	TM_{010}	TE_{011}
Frequency (MHz)	1467	2824
Geometry factor $G = R_s Q_0$ (Ω)	273	701
$E_p/\sqrt{U}$ [MV/(m$\sqrt{\mathrm{J}}$)]	17	0
$B_p/\sqrt{U}$ (mT/J)	43	50
A_{eff} (m^2)	0.0586	0.0320

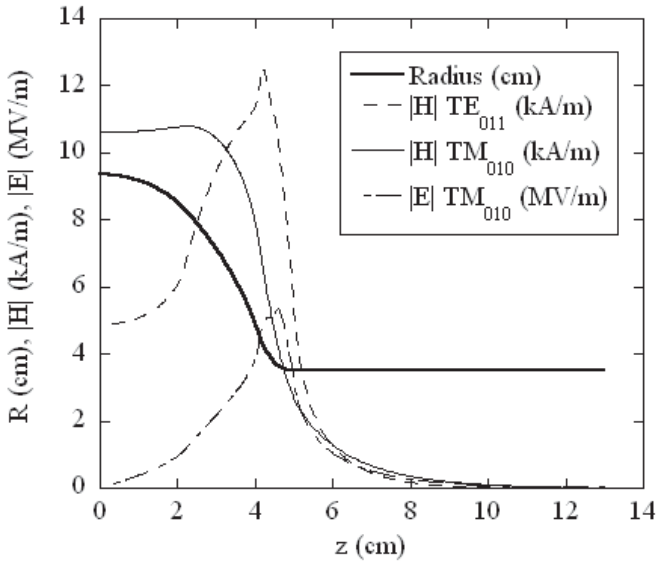

FIG. 1. Surface fields for the TE_{011} and TM_{010} modes for 50 mJ cavity stored energy.

side wall and iris region, where the electric field is high in the TM_{010} mode.

The input and output loop couplers couple to the magnetic field of the cavity mode. They are inserted in cylindrical side ports close to the cavity irises (Fig. 2). Their size has been determined experimentally by ''trial and error'' and the orientation is such that the plane of the loop is parallel to the cavity equatorial plane. The Q_{ext} of the input coupler is about 2×10^{10} for the TM_{010} mode and 1×10^{10} for the TE_{011} mode while the Q_{ext} of the output coupler is about 7×10^{10} for the TM_{010} mode and 4×10^{10} for the TE_{011} mode.

The standard cavity preparation for rf test at 2 K consists of the following:

(i) ultrasonic degreasing for 20 min;

(ii) buffered chemical polishing (BCP) with HNO_3, HF, H_3PO_4 (1:1:1) at 25 °C removing about 20 μm of niobium from the inner cavity surface, after initial removal of about 130 μm after the cavity fabrication;

(iii) high-pressure rinsing (HPR) with ultrapure water at a pressure of 80 bar for 1 h;

(iv) drying overnight in class 10 clean room;

(v) assembly of beam pipe niobium flanges with indium wire 1.52 mm thick as gasket and input and output loop couplers in class 10 clean room;

(vi) the cavity is attached to a test stand and evacuated to about 10^{-8} mbar prior to cool-down to 2 K.

Figure 2 shows a picture of the cavity assembled on the test stand. The cavity side ports have Nb55Ti $2\frac{3}{4}''$ Conflat flanges while the loop couplers have stainless steel Conflat flanges and a copper gasket is used for seal. This design showed to be very reliable, since no leaks were detected in superfluid helium after about 20 thermal cycles from room temperature to 2 K.

FIG. 2. (Color) CEBAF single-cell cavity with side-port loop couplers attached to the vertical test stand.

B. Measurements with BCP-treated cavity

Figure 3 shows the result of the cavity high-power test at 2 K in the TM_{010} and TE_{011} mode before and after baking the cavity under vacuum at 100 °C for 48 h flowing hot

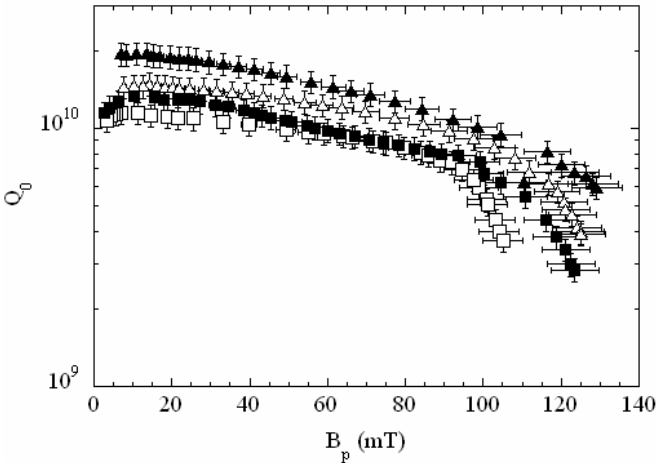

FIG. 3. Q_0 vs B_p in the TM_{010} mode (squares) and TE_{011} mode (triangles) at 2 K after a new surface preparation (open symbols) and after baking at 100 °C for about 48 h (solid symbols). The cavity was limited by quench after baking.

nitrogen on the cavity outer surface. The TM_{010} mode shows a sharp decrease of the quality factor starting at $B_p = 90$ mT without field emission while the TE_{011} mode shows a smoother drop up to $B_p = 125$ mT where the cavity quenched. The quality factor at low field improved in both modes after baking and in the TM_{010} mode the maximum field increased up to 124 mT in the absence of field emission but the Q drop is still present. A brief multipacting activity was found at about $B_p = 100$ mT in the TM mode. The quality factor at high field in the TE mode improved by baking, most probably due to the reduction of the BCS surface resistance, as will be discussed in Sec. III. The cavity was subsequently baked at higher temperature (120 °C, 48 h) but no improvement was obtained in either mode.

The low-field ($B_p \approx 10$ mT) surface resistance as a function of the He bath temperature was measured in both modes, before and after baking, and the data were fitted [8] with the sum of the T-independent residual resistance, R_{res}, and the Bardeen-Cooper-Schrieffer (BCS) surface resistance [9]. The fitting parameters were the normal electrons' mean free path, l, the energy gap at 0 K divided by the critical temperature, Δ/kT_c, and R_{res}. The critical temperature ($T_c = 9.25$ K), coherence length ($\xi = 39$ nm) and the penetration depth at 0 K ($\lambda = 32$ nm) are considered material constants for niobium. A plot of R_s as a function of $1/T$ for both modes before and after baking at 100 °C for about 40 h is shown in Fig. 4. The BCS surface resistance decreased by about 30% in both modes while the residual resistance increased by about 5 nΩ by baking, consistent with previous studies [10–12].

After the rf tests, the inner surface of the cavity was visually inspected and two "black spots" of a millimeter size were seen on the walls, in the area of high magnetic field for the TE mode. Since they were suspected to be the cause of the quenches, they were mechanically ground away with a carbide tool.

1. Anodization

After a new chemical etching of about 50 μm with BCP 1:1:1, the cavity was anodized by filling it with ammonium hydroxide (NH_4OH) 30% diluted and applying a constant voltage between the cavity (anode) and a niobium rod (cathode) inserted in the cavity. This process grows a niobium pentoxide layer on the cavity surface at a rate of about 2 nm/V [13]. The cavity was processed at 45 V, 1 A (current density of about 1 mA/cm^2) until the current dropped to about 100 mA, growing a Nb_2O_5 layer about 90 nm thick (about 50 times thicker than the natural oxide grown without anodization).

The rf test at 2 K did not show a significant difference from the previous ones: the Q drop starts at about $B_p = 95$ mT in both modes. The cavity was baked in the cryostat with hot helium up to 115 °C for about 40 h. The maximum field in the TM_{010} mode improved by about 16% with some residual Q drop while the TE_{011} mode quenched at $B_p = 102$ mT. The BCS surface resistance decreased by about 42% in both modes while the residual resistance increased by about 2 nΩ. Figure 5 shows a plot of Q_0 vs B_p for both modes before and after baking. The low-field quality factor is lower than usually measured due to higher residual resistance. It was found that the reason for it was a current drift in the power supply of the compensation coil which shields the Earth's magnetic field. The residual field was measured to be about 20 mG, corresponding to about 6 nΩ of additional residual resistance.

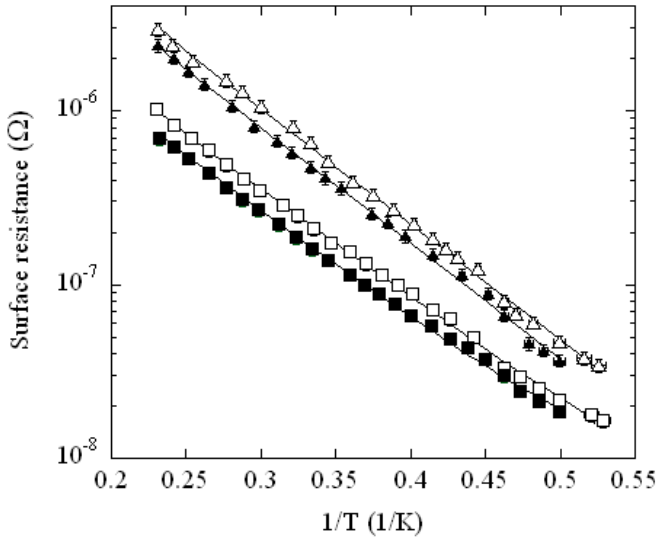

FIG. 4. R_s vs $1/T$ for the TM_{010} (square) and TE_{011} modes (triangles) before (open symbols) and after (solid symbols) baking at 100 °C for about 40 h. Data points are fitted with the BCS theory plus residual resistance (solid lines).

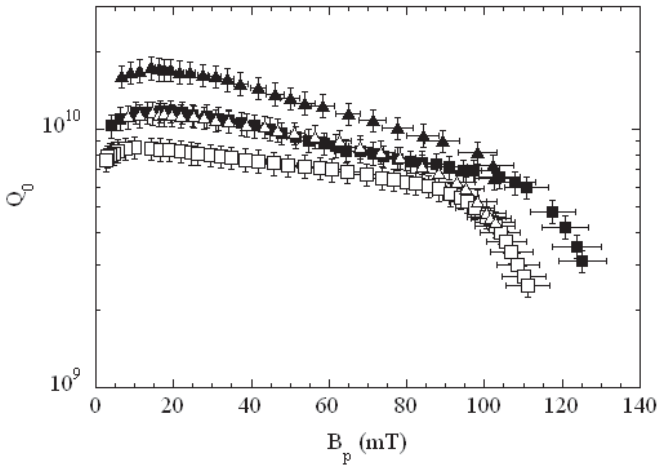

FIG. 5. Q_0 vs B_p in the TM_{010} mode (squares) and TE_{011} mode (triangles) at 2 K after anodization (open symbols) and after baking at 115 °C for about 40 h (solid symbols). The cavity was limited by quench in the TE mode.

2. Postpurification

One way to increase the quench field of a cavity is to improve the thermal conductivity of the niobium. This can be accomplished by heat treating the cavity in a vacuum furnace at 1250 °C in the presence of titanium as a solid state getter material. The treatment followed the recipe developed in Ref. [14]: the temperature is raised to 1250 °C in about 4 h and is held for 12 h, allowing the titanium to sublimate and deposit on the niobium cavity. The temperature is then lowered to 1000 °C at a rate of $-0.2\,^{\circ}\mathrm{C}/\mathrm{min}$ and the purification of the niobium occurs. After reaching 1000 °C, the cool-down to room temperature began and took about 9 h. The maximum pressure was about 10^{-4} mbar at 1250 °C, decreasing to about 10^{-7} mbar before cool-down. The main gas species detected by the residual gas analyzer were hydrogen, nitrogen and water. As an indication of the effectiveness of the process, the residual resistivity ratio (RRR) of a niobium sample was measured before and after the postpurification: it improved from 390 to 720. During the postpurification process, the niobium homogenizes and recrystallizes to large (millimeter-size) grains.

Following postpurification, about 95 μm were removed from the inner cavity surface by BCP 1:1:1 and the results of the rf test at 2 K showed about 20% increase in the onset of the Q drop in both modes (110 mT in the TM_{010} mode, 120 mT in the TE_{011} mode). The cavity was *in situ* baked with hot helium in the cryostat at 120 °C for about 30 h. The test results after baking showed a recovery from the Q drop in both modes but the TE_{011} quenched at the same field as before baking ($B_p = 145$ mT) while the maximum field in the TM_{010} increased by 13% (up to 135 mT). The residual resistance increased 7 nΩ in the TM_{010} mode while it did not change in the TE_{011} mode. Figure 6 shows the Q_0 vs B_p curves at 2 K before and after baking. The

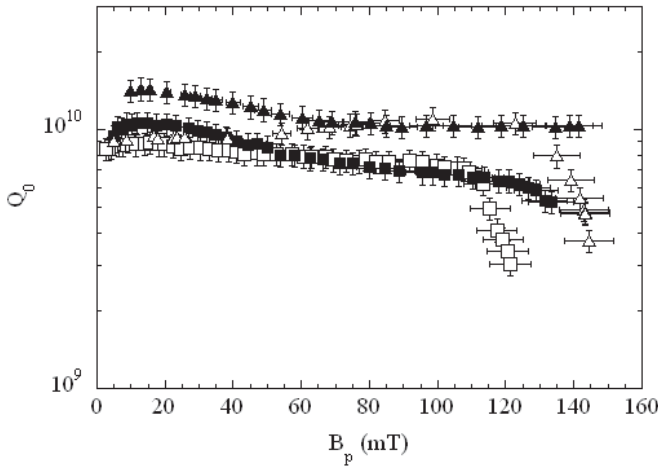

FIG. 6. Q_0 vs B_p in the TM_{010} mode (squares) and TE_{011} mode (triangles) at 2 K after postpurification (open symbols) and after baking at 120 °C for about 30 h (solid symbols). The cavity was limited by quench after baking.

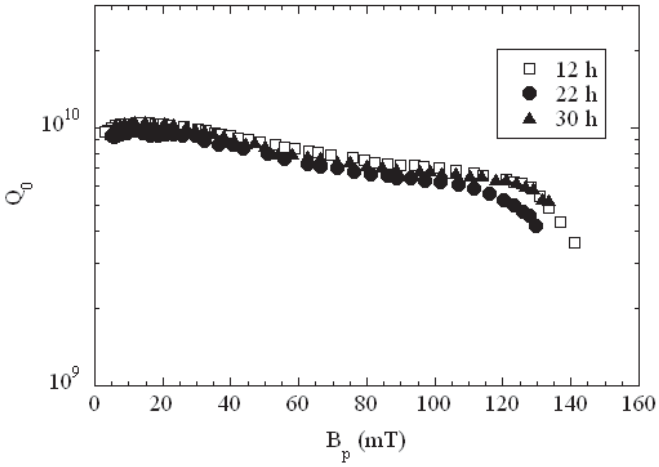

FIG. 7. Summary of Q_0 vs B_p at 2 K for the TM_{010} mode after postpurification and baking at 115 °C for different durations. A new surface preparation with BCP was done after each test and the Q drop began between 92–110 mT prior to baking. The data after baking for 30 h are shown also in Fig. 6.

cavity was tested again after a new surface preparation and baked afterwards at 115 °C for 22 h and the results confirmed the ones shown in Fig. 6.

In a study of the effect of the low-temperature baking [12] it was found that the baking temperature which allows the largest reduction in the BCS surface resistance and a recovery from the Q drop is 120 °C. The baking time was kept fixed at 48 h. In this series of tests we reduced the baking time down to 12 h, keeping the temperature at 115–120 °C and we found similar reductions of the Q drop for baking time between 12 and 48 h, as shown in Fig. 7.[1] Visentin recently showed that baking at 100 °C for only 3 h gives only a marginal improvement of the Q drop [15]. The effect of baking time on the BCS surface resistance is shown in Fig. 8, with larger reduction occurring for baking time up to 48 h and consistent with a previous study by Kneisel at 145 °C [10].

III. COMPARISON OF MODELS

The average values of the material parameters, in a 40 nm depth from the niobium surface, before and after baking are shown in Table II. Those values are consistent with the ones reported in Ref. [12] and the strong reduction of the mean free path by baking suggests a diffusion of impurities from the surface towards the bulk as the main process occurring during bakeout. The reduction of the BCS surface resistance is accomplished by the reduction of the mean free path and the slight increase (about 6%) of Δ/kT_c. The causes for the increases of Δ/kT_c and of R_{res} are not yet clear. A possible explanation for the higher R_{res} could be the enhancement of the metal/oxide interface

[1] A new surface preparation by BCP was done prior to each baking.

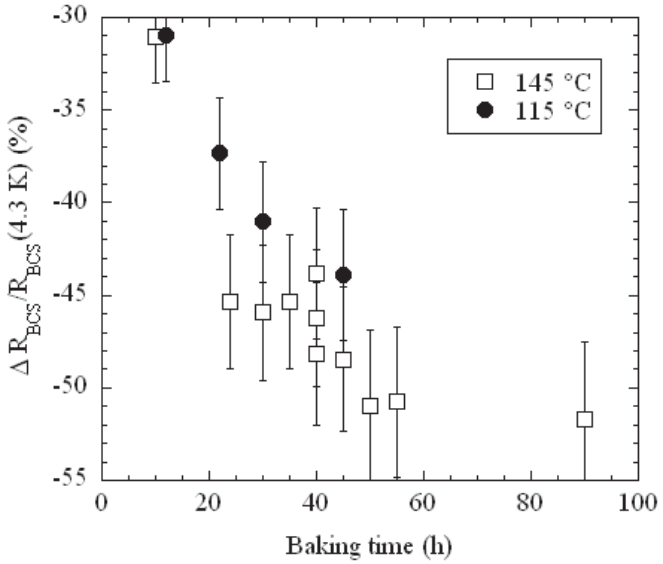

FIG. 8. Variation of the BCS surface resistance at 4.3 K after baking at 115 °C (solid circles) for different amount of time, compared with data from Kneisel 10 at 145 °C (open squares).

losses, as proposed by Halbritter [16], or an increase of magnetic impurities as indicated in Ref. [17]. The reduction of the mean free path by baking indicates that the surface resistance changes from clean ($l > \xi$) to dirty ($l < \xi$) limit and therefore the development of a theoretical treatment of the BCS surface resistance at low temperature ($T/T_c < 0.23$) and high rf field ($B_{rf}/B_c > 0.5$) as a function of the mean free path could be very useful, as already pointed out in Ref. [4].

Regarding the high-field losses, the most important experimental evidence shown here is given by the presence of the Q drop and its elimination by baking in the TE_{011} mode, where only magnetic field is present on the cavity surface. In the following, the experimental results are compared with different Q-drop models.

A. Thermal feedback model

A possible explanation for the Q drop is the so-called thermal feedback model (TFBM), outlined in detail in Ref. [4]. According to this model, the Joule heating generated at the cavity inner surface due to the rf field cannot be completely dissipated in the He bath, due to the limited thermal conductivity of the niobium and of the Kapitza resistance at the Nb/He interface. Consequently, the BCS surface resistance increases, due to its exponential dependence on temperature, causing even higher dissipated power and such positive feedback lowers the quality factor and ultimately causes a thermal breakdown of the cavity. As part of the model, an intrinsic increase of the BCS surface resistance at higher field due to pair-breaking effects is introduced. Figure 9 shows a plot of Q_0 vs B_p for both TE_{011} and TM_{010} data before postpurification and baking, compared with the prediction of the TFBM model

TABLE II. Values of material parameters for the TM_{010} and TE_{011} before and after baking at 100–120 °C for 12–48 h averaged over several rf tests.

	TM_{010} mode		
	Δ/kT_c (40 mm)	l (40 nm) (nm)	R_{res} (nΩ)
Baselines	1.725 ± 0.007	93 ± 12	6.7 ± 0.1
100–120 °C	1.824 ± 0.003	27 ± 37	15.2 ± 0.2
	TE_{011} mode		
	Δ/kT_c (40 mm)	l (40 nm) (nm)	R_{res} (nΩ)
Baselines	1.760 ± 0.006	120 ± 23	10.2 ± 0.3
100–120 °C	1.793 ± 0.008	31 ± 11	13.5 ± 0.9

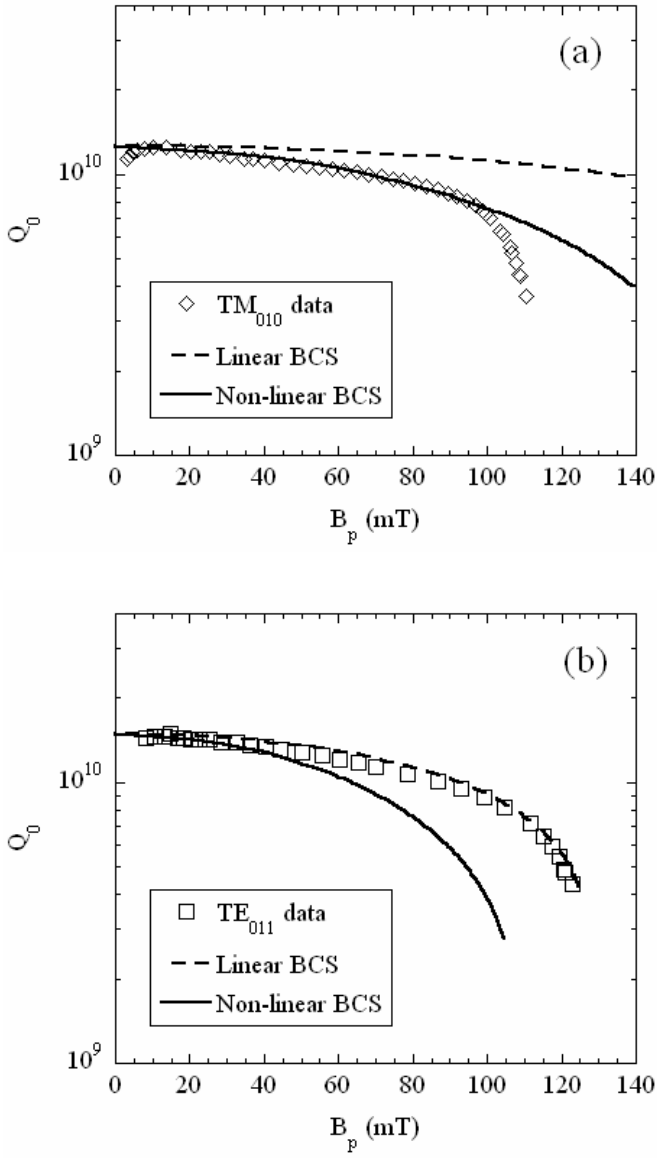

FIG. 9. Q_0 vs B_p data compared with the TFBM model with and without nonlinear correction to the BCS surface resistance at 2 K for both TM_{010} (a) and TE_{011} modes (b).

with and without the nonlinear pair-breaking correction to the BCS surface resistance. The thermal conductivity and Kapitza resistance of RRR $\approx$ 300 niobium were taken from Refs. [4,18], respectively.

Figure 9 shows that the TFBM model does not predict the Q drop in the TM mode, while it describes it well in the TE mode, without the nonlinear contribution. Therefore, the Q drop in the TE mode before postpurification is due most likely to ''global heating'' because of the higher frequency than in the TM mode ($R_s \propto f^2$) and its reduction by baking (Fig. 3) could be due to the lower BCS surface resistance. On the other hand, the Q drop cannot be described by the TFBM with higher thermal conductivity after postpurification as shown in Fig. 10. The thermal conductivity and Kapitza resistance of RRR $\approx$ 700 niobium were taken from Refs. [4,19], respectively. The fact that the nonlinear BCS does not describe well the experimental data for the TE mode indicates that the frequency dependence of the pair-breaking term might be overestimated, as suggested also by data on cavities at 3.9 GHz [4].

B. Magnetic field enhancement model

Another model which tries to explain the cause of the Q drop is the so-called magnetic field enhancement model (MFE), described in detail in Ref. [7]. The model considers the geometric magnetic field enhancement caused by sharp corners, especially at grain boundaries, on the cavity surface. The edge of a grain boundary can become normal conducting because the local magnetic field, enhanced by a factor β_m, exceeds the thermodynamic critical field. This causes a progressive reduction of the quality factor as more boundaries become normal conducting at higher fields.

TABLE III. Average values of the fitting parameters β_0 and σ of the MFE model for the TM_{010} and TE_{011} mode at 2 K before and after baking for different cavity treatments.

	TM_{010}		TE_{011}	
	β_0	σ	β_0	σ
Before baking	1.49	0.0060	1.21	0.0070
After 100–120 °C bake	1.19	0.0072	···	···
Anodization	1.42	0.0070	1.48	0.0070
After 115 °C bake	1.14	0.0075	···	···
Postpurification	1.64	0.0067	1.4	0.0070
After 115–120 °C bake	1.32	0.0075	···	···

The grain boundary size (taken to be 50 μm and 1 mm before and after postpurification, respectively), the center of the distribution of field enhancement factors, β_0, and the width of the distribution, σ, are parameters of the model. The values of β_0 and σ obtained from a fit of the model with the TM and TE mode data are shown in Table III and they are consistent with the ones reported in Ref. [7]. Although the model describes well the data before baking, as shown in Fig. 11, the reduction of Q drop by baking would be explained by a decrease of the geometric field enhancement factor, which could be hardly justified since the baking temperature is low enough to cause any change of the surface topography.

C. Interface tunnel exchange model

Finally, the so-called interface tunnel exchange (ITE) model proposed in Refs. [2,3] explains the Q drop as being due to the presence of an oxide layer with a high density of localized states which allows resonant tunneling of elec-

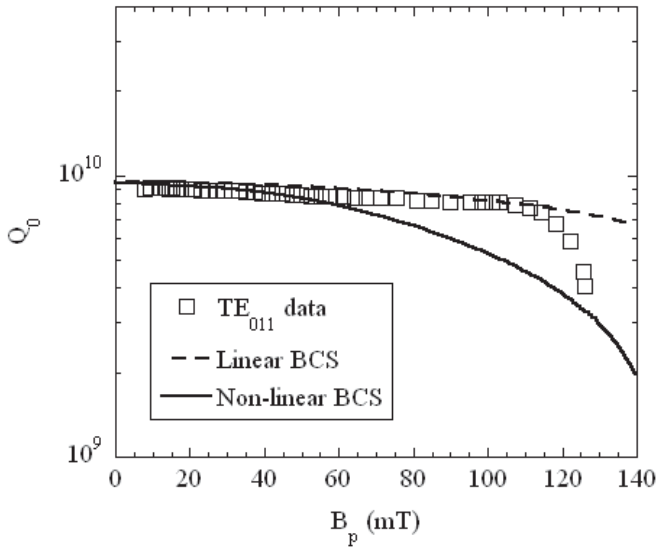

FIG. 10. Q_0 vs B_p data compared with the TFBM model with and without nonlinear correction to the BCS surface resistance at 2 K after postpurification for the TE_{011} mode.

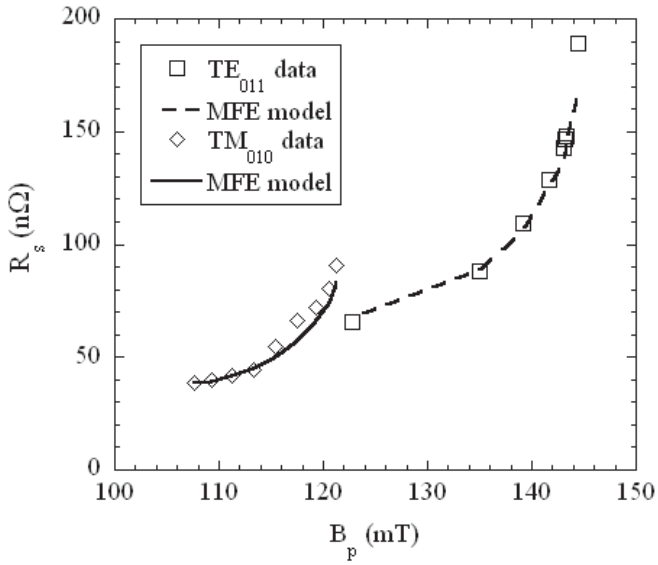

FIG. 11. High-field R_s vs B_p data at 2 K compared with the MFE model.

TABLE IV. Average values of the parameters b, E_0, c, and correlation factor for the ITE model compared with Q-drop data at 2 K for the TM_{010} mode for different cavity treatments. In some cases, the value of E_0 could not be obtained because the additive constant $-be^{-c/E_0}$ of Eq. (2) turned out to be positive from the fit.

	b (Ω)	c (MV/m)	E_0 (MV/m)	r^2
Before baking	105	959	···	0.998
After 100–120 °C bake	18.6	952	41.1	0.997
Anodization	0.40	727	···	0.999
After 115 °C bake	5.80	990	45	0.998
Postpurification	33.3	952	40.8	0.994
After 115–120 °C bake	0.02	867	49.2	0.966

trons between conduction levels in the metal and localized states for sufficiently high electric fields. This additional contribution to the surface resistance at high fields, R_s^E, has an exponential dependence to the peak surface electric field:

$$R_s^E = b(e^{-c/E_p} - e^{-c/E_0}), \tag{2}$$

where b is proportional to the oxide thickness and the density of localized states, c depends on tunneling distance, energy gap, dielectric constant and a field enhancement factor. E_0 is the onset field for the Q drop. The average values of b, E_0, and c obtained from a fit of the data for the TM_{010} mode before and after baking for different cavity treatments are shown in Table IV. The values of c and E_0 are consistent with those reported in Ref. [12] and the exponential dependence well describes the data, as shown in Fig. 12.

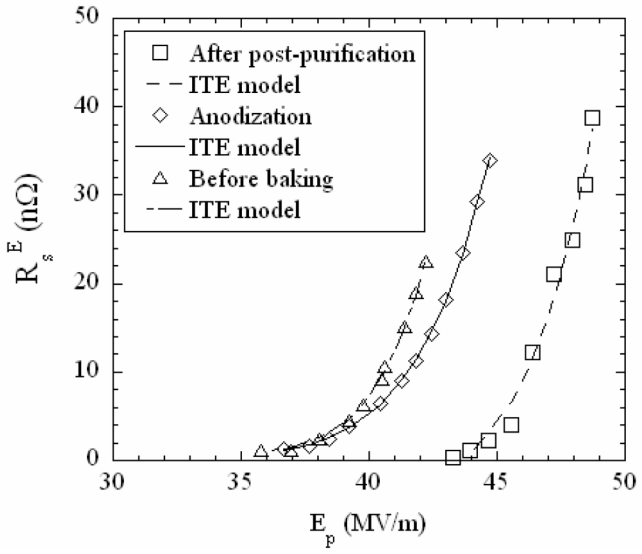

FIG. 12. R_s^E vs E_p at 2 K for the TM_{010} mode and for different cavity treatments before baking compared with the ITE model.

IV. DISCUSSION

The data presented in this contribution show that the Q drop is present in the TE_{011} mode, which has zero electric field on the surface, as well as in the TM_{010} mode and that the presence of an oxide layer much thicker than the one formed naturally by the oxidation of niobium in air does not change significantly the onset of the Q drop. These results are in contradiction with the predictions of the ITE model. Furthermore, recent experimental data show that the Q drop does not reappear in a baked cavity after the oxide layer is stripped by HF treatments and a new one is formed [15]. Therefore there is sufficient experimental evidence to indicate that the Q drop is not caused by the niobium oxide layer.

The TFBM does not provide a good description of the experimental data at high field, as shown also in Ref. [4]. The MFE model is in good agreement with the data but does not provide a physical explanation for the reduction of the Q drop by baking or the presence of the Q drop on cavity with much smoother surfaces, such as those treated by electropolishing [20] or made of single crystal [21].

The dependence of the material parameters on the baking time and temperature suggest an impurity diffusion process occurring during bakeout. The only impurity present in noticeable quantities in niobium which has a diffusion length comparable to the rf penetration depth for the usual baking parameters is oxygen. New models [22,23] link the presence of interstitial oxygen near the metal/oxide interface to a reduction of the surface barrier, allowing fluxons to penetrate at a reduced lower critical field, B_{c1}. Baking would allow a redistribution of oxygen, creating a more uniform ''contaminated'' layer with higher B_{c1}. Rabinowitz [24] was able to estimate the power loss due to a single isolated fluxoid trapped near the surface of a superconductor in the presence of rf field. He predicts an exponential dependence of the surface resistance on the peak magnetic field, above the onset of flux penetration, which well describes the experimental data. The data also show that the onset of the Q drop in the TE mode is higher than in the TM mode and this is compatible with the hypothesis of delayed flux penetration by the higher frequency of the rf field [25].

V. CONCLUSIONS

The experimental results presented in Sec. II show that high-field losses characterized by a sudden exponential increase of the surface resistance as a function of the peak surface magnetic field, in absence of field emission, are present both in the TM_{010} mode as well as in the TE_{011} mode, under the same surface conditions. This suggests that the magnetic, rather than the electric field is responsible for the additional losses. The data cannot be described by a ''global'' uniform heating of the surface (TFBM model). This became clear for the TE_{011} mode also once the thermal conductivity of the niobium was improved by postpurification.

Other models (ITE and MFE) provide good numerical description of the data but lack a good physical explanation for some of the results such as the drastic reduction of the Q drop by baking and the presence of the Q drop in the TE_{011} mode. Models based on reduced surface barrier by oxygen contamination seem promising to explain the Q drop and the baking effect but need further experimental and theoretical investigation.

ACKNOWLEDGMENTS

We would like to thank B. Manus, G. Slack, and J. Brawley for helping with the cavity fabrication, B. Golden and D. Forehand for helping with the high-pressure rinsing and the cavity heat treatment, and P. Kushnick for cryogenic support. This work was supported by the U.S. DOE Contract No. DE-AC05-84ER40150 Modification No. M175, under which the Southeastern Universities Research Association (SURA) operates the Thomas Jefferson National Accelerator Facility.

[1] B. Visentin, in *Proceedings of the 11th Workshop on RF Superconductivity, Travemunde, 2003*, edited by D. Proch (DESY, Hamburg, Germany, 2004), p. TuO01.
[2] J. Halbritter, Z. Phys. B **31**, 19 (1978).
[3] J. Halbritter, P. Kneisel, V. Palmieri, and M. Pekeler, IEEE Trans. Appl. Supercond. **11**, 1864 (2001).
[4] P. Bauer, G. Ciovati, G. Eremeev, A. Gurevich, L. Lilje, N. Solyak, and B. Visentin, Physica C (Amsterdam) (to be published).
[5] R. M. Sundelin, IEEE Trans. Nucl. Sci. **32**, 3570 (1985).
[6] J. H. Billen and L. M. Young, Los Alamos National Laboratory Report No. LA-UR-96-1834, 2004.
[7] J. Knobloch, R. L. Geng, M. Liepe, and H. Padamsee, in *Proceedings of the 9th Workshop on RF Superconductivity, Santa Fe, 1999*, edited by F. Krawczyk (LANL, Los Alamos, NM, 2000), p. 77.
[8] G. Ciovati, Jefferson Lab Report No. JLAB-TN-03-003, 2003.
[9] J. Halbritter, Forschungszentrum Karlsruhe, FZK 3/70-6, 1970.
[10] P. Kneisel, in *Proceedings of the 9th Workshop on RF Superconductivity, Santa Fe, 1999* (Ref. [7]), p. 328.
[11] B. Visentin, J. P. Charrier, and G. Congretel, in *Proceedings of the 2001 Particle Accelerator Conference, Chicago, 2001*, edited by P. W. Lucas and S. Webber (FNAL, Batavia, IL, 2001), p. 1056.
[12] G. Ciovati, J. Appl. Phys. **96**, 1591 (2004).
[13] L. Young, *Anodic Oxide Films* (Academic Press, New York, 1961).
[14] H. Safa, D. Moffat, F. Koechlin, E. Jacques, and Y. Boudigou, in *Proceedings of the 7th Workshop on RF Superconductivity, Gif sur Yvette, 1995*, edited by B. Bonin (IN2P3, Orsay, France, 1995), p. 649.
[15] B. Visentin, in *Proceedings of the Pushing the Limits of RF Superconductivity Workshop, Argonne, 2004*, edited by K.-J. Kim and C. Eyberger (ANL, Argonne, IL, 2005), p. 94.
[16] J. Halbritter, in *Proceedings of the 38th Eloisatron Workshop, Erice, 1999*, edited by L. Cifarelli and L. Maritato (University of Salerno, Salerno, Italy, 2001), p. 9.
[17] S. Casalbuoni, E. A. Knabbe, J. Kotzler, L. Lilje, L. von Sawilski, P. Schmuser, and B. Steffen, Nucl. Instrum. Methods Phys. Res., Sect. A **538**, 45 (2005).
[18] S. Bousson, M. Fouaidy, T. Junquera, N. Hammoudi, J. C. Le Scornet, and J. Lesrel, in *Proceedings of the 9th Workshop on RF Superconductivity, Santa Fe, 1999* (Ref. [7]), p. 263.
[19] J. Amrit, C. Z. Antoine, M. X. Francois, and H. Safa, in *Advances in Cryogenic Engineering: Proceedings of the Cryogenic Engineering Conference*, edited by Susan Breon *et al.*, AIP Conf. Proc. No. 613 (AIP, New York, 2002), Vol. 47, p. 499.
[20] L. Lilje, D. Reschke, K. Twarowski, P. Schmuser, D. Bloess, E. Haebel, E. Chiaveri, J.-M. Tessier, H. Preis, H. Wenninger, H. Safa, and J. P. Charrier, in *Proceedings of the 9th Workshop on RF Superconductivity, Santa Fe, 1999* (Ref. [7]), p. 74.
[21] P. Kneisel, G. R. Myneni, G. Ciovati, J. Sekutowicz, and T. Carneiro, in *Proceedings of the 2005 Particle Accelerator Conference, Knoxville, 2005*, edited by C. Horak (ORNL, Oak Ridge, TN, 2005), p. 3991.
[22] H. Safa, in *Proceedings of the 10th Workshop on RF Superconductivity, Tsukuba, 2001*, edited by S. Noguchi *et al.* (KEK, Tsukuba, Japan, 2003), p. 279.
[23] G. Ciovati, Ph.D. thesis, Old Dominion University, 2005.
[24] M. Rabinowitz, J. Appl. Phys. **42**, 88 (1971).
[25] M. Rabinowitz, Appl. Phys. Lett. **19**, 73 (1971).